

## CHANGE OF THE ANTIMONY ANODIZING KINETICS BY COATING THE ELECTRODE WITH A THIN FILM

Emil Lilov<sup>1</sup>, Vanya Lilova<sup>1</sup>, Svetlozar Nedev<sup>1</sup>, Stephan Kozhukharov<sup>1,2</sup>,  
Alaa M. Adam<sup>3</sup>, Christian Girginov<sup>4</sup>

<sup>1</sup>Department of Physics, University of Chemical Technology and Metallurgy  
8 Kliment Ohridski Blvd., 1756, Sofia, Bulgaria

<sup>2</sup>LAMAR – Laboratory for Advanced Materials Research  
University of Chemical Technology and Metallurgy  
8 Kliment Ohridski Blvd., 1756, Sofia, Bulgaria

<sup>3</sup>Physics Department, Faculty of Science  
Sohag University, 82524, Sohag, Egypt

<sup>4</sup>Department of Physical Chemistry  
University of Chemical Technology and Metallurgy  
8 Kliment Ohridski Blvd., 1756, Sofia, Bulgaria  
E-mail: emo.lilov@uctm.edu

Received 06 February 2023  
Accepted 28 February 2023

---

### ABSTRACT

The present research work is dedicated on the processes kinetics description of the antimony anodization in potassium phosphate ( $K_3PO_4$ ) aqueous solutions. The data have shown that the slope of the kinetic curves is dependent on the phosphate solution concentration. Besides, their mathematic approximation has revealed occurrence of a critical phosphate solution concentration of  $0.11 \text{ mol dm}^{-3}$ . At this concentration, the slope of the kinetic curve tends to zero. Above this critical concentration, induction periods occur during the anodization. Additional experiments were performed with thin  $Sb_2O_3$  layers preliminary deposited in vacuum. This approach has enabled to define the impact of such layers on the kinetic behavior during the anodization process. The results have shown that various stages of the process could be skipped. The final data analysis has confirmed the suggestion that the induction periods and voltage variations during the anodization process are caused by the formation of a thin  $Sb_2O_3$  film, whose dielectric properties change with the film thickness increment.

*Keywords:* anodization of antimony, potassium phosphate, antimony oxide, vacuum thermal evaporation, induction periods.

---

### INTRODUCTION

The anodizing of antimony in aqueous and nonaqueous solutions of acids, alkalis, and salts has been extensively studied [1 - 5]. The increased interest in the anodic behavior of antimony is due to its use in lithium-ion and sodium batteries [6 - 13] and analytical determinations [14, 15]. Induction periods are observed during anodizing under certain conditions [16] and their duration decreases with increasing current density according to a power law [17]. There are suggestions in the literature that low-impedance semiconductor layers form during induction periods in aqueous solutions of phosphoric acid [18] analogous to the induction periods

during anodizing of molybdenum [19]. According to the voltammetric and ellipsometric data, the anodic behavior is a stepwise electroformation of different antimony species, with  $Sb_2O_3$  being the final product [20]. It was determined in reference [21] that induction periods are a common phenomenon when anodizing antimony in various electrolytes. In another study on anodizing antimony in aqueous solutions of oxalic acid [22], an increase in layer dissolution was observed with an increase in electrolyte concentration, which accounts for the occurrence of these induction periods. However, the nature of the induction periods and the “hump” that appears in some kinetic curves are not yet fully understood. This work aims to provide an experiment

that will help to understand the nature of the induction periods and the “hump” that occurs during the anodizing of antimony.

## EXPERIMENTAL

Antimony electrodes (99.999 % pure) were cut into cylindrical pieces. The working surface was one of the cylinder’s bases with an area of 0.8 cm<sup>2</sup>, which was mechanically polished using a polishing paste with grain sizes of 0.5 μm. The remaining cylinder surfaces were sealed with epoxy resin. The electrodes were anodized in a standard two-electrode cell, using a gold cathode in galvanostatic mode with a current density of 5 mA cm<sup>-2</sup> and a temperature of 293 K. The continuations of the anodization processes were extended up to 330 s, in accordance either with the induction period duration or breakdown voltage achievement.

The forming electrolytes were aqueous solutions of K<sub>3</sub>PO<sub>4</sub> with concentrations ranging from 0.001 to 0.12 mol dm<sup>-3</sup>. The kinetic curves were sampled by acquisition of 2 data points per second, during the anodization processes. The used data acquisition device was Peak Tech 4000 digital multimeter, combined by commercial PC for data collection.

For the purpose of the present research work, another set of antimony electrodes with preliminary vacuum deposited Sb<sub>2</sub>O<sub>3</sub> films was used. The oxide films were obtained by vacuum deposition from Sb<sub>2</sub>O<sub>3</sub> source (with 99 % of purity, provided by Alfa Aesar, Cas No: 1309-64-4). It was vacuum-thermally evaporated by tantalum evaporator filled with quartz wool. The Sb<sub>2</sub>O<sub>3</sub> film thickness varied from 7 to 100 nm, in accordance with the amounts of Sb<sub>2</sub>O<sub>3</sub> loading. The film thickness values were measured using a Talystep Taylor-Hobson profiler, on a glass plate positioned near the sample. The distance between the evaporator and the substrate was 15 cm in order to keep the substrates at room temperature.

## RESULTS AND DISCUSSION

The slope of the kinetic curve decreases with the increase in the electrolyte concentration, temperature, and current density reduction [23]. The dependence of the measured potential increment (**dU**) on the electric charge quantity (**dQ**) kinetic curves were acquired by galvanostatic anodization of Sb electrodes in K<sub>3</sub>PO<sub>4</sub>

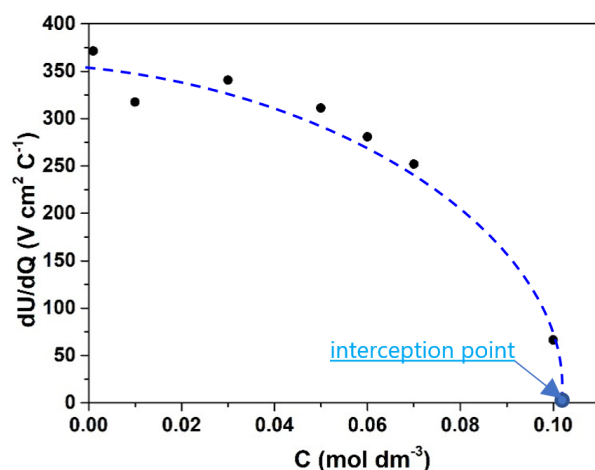


Fig. 1. Dependence of the kinetic curves slopes on the concentration of the electrolyte for anodizing of antimony in aqueous solutions of K<sub>3</sub>PO<sub>4</sub>.

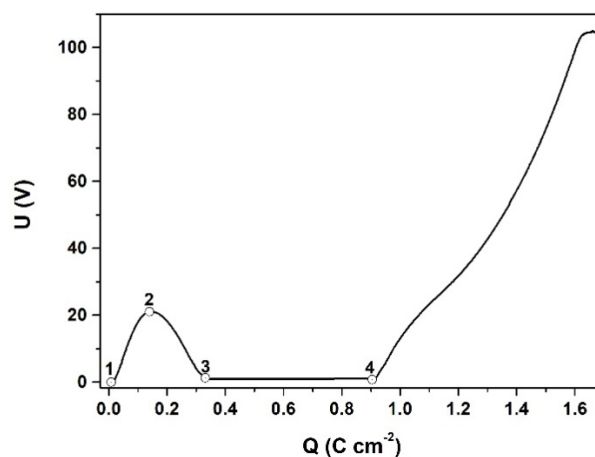


Fig. 2. Kinetic curve for anodizing of antimony (not coated with Sb<sub>2</sub>O<sub>3</sub>) in a 0.12 mol dm<sup>-3</sup> aqueous solution of K<sub>3</sub>PO<sub>4</sub>.

aqueous solutions at a constant current density of 5 mA cm<sup>-2</sup>. The electrolyte concentrations were selected in a wide concentration range, as follows: 10<sup>-3</sup>; 10<sup>-2</sup>; 3x10<sup>-2</sup>; 5x10<sup>-2</sup>; 6x10<sup>-2</sup>; 7x10<sup>-2</sup> and 0.1 mol dm<sup>-3</sup>. The kinetic curve slope values, obtained by the respective anodizations were summarized and represented in function of the respective concentrations, as it is shown in Fig. 1.

The dependence on the electrolyte concentration, when approximated by a second-degree polynomial, crosses the abscissa at around 0.11 mol dm<sup>-3</sup>, (noticed as interception point in Fig. 1) and an induction period appears immediately after this concentration (Fig. 2).

The X-axis represents the charge density,  $Q = j \cdot t$ , where  $j$  is the current density in  $\text{mA cm}^{-2}$  and  $t$  is the anodizing time in seconds. Besides, a “hump” is observable, where the voltage increases at the beginning of the anodizing process (section 1 - 2), reaches a maximum (point 2), then decreases back to around 0.9 V (point 3), and remains relatively constant until the end (point 4), of the induction period (section 1-4).

In cases of Sb electrodes preliminary coated by thin  $\text{Sb}_2\text{O}_3$  layer the anodizing process kinetics is different (as shown in Figs. 3, 4, and 5). If the coating thickness is 7 nm (Fig. 3), then the hump in the kinetic curve decreases significantly, from 60 s for the uncoated electrode to only 2 to 3 s for the coated one. The hump maximum voltage also changes, decaying from above 20 V for the uncoated electrode to less than 1 V for the coated one.

This hump completely disappears at higher  $\text{Sb}_2\text{O}_3$  layer thickness, as it is demonstrated in Fig. 4.

The experiments have revealed that the thicker  $\text{Sb}_2\text{O}_3$  layers result in shortening of the induction periods during the anodization of the respective samples, as is shown in Fig. 5.

At higher thicknesses, the induction period may even become negligible, as depicted in Fig. 6.

The change in the kinetics of anodizing may be attributed to variations in the properties of the resulting film. A correlation between the band gap width and film thickness has been established for some materials [24 - 27]. A reduction in thickness to less than 10 nm can lead to an increase in the band gap due to quantum confinement and amorphous effects [24]. This phenomenon of band gap width reduction with increasing layer thickness has been observed for anodic films on zinc [28]. Additionally, a dependence of the kinetic curve slope and the layer band gap width on electrolyte concentration was found [29].

At the start of anodizing, when the film thickness grows from zero to a certain value, the layer's specific resistance is high due to the large band gap, causing an increase in the formation voltage. Upon reaching a certain thickness, the band gap width starts to decrease, leading to a reduction in specific resistance and voltage drop, resulting in a hump on the kinetic curve. At this stage (point 3 in Fig. 2), the electronic current is very high, the ionic current is very low, the film growth and dissolution are almost equal, and the film thickness increases very slowly. After point 4 (Fig. 2), the

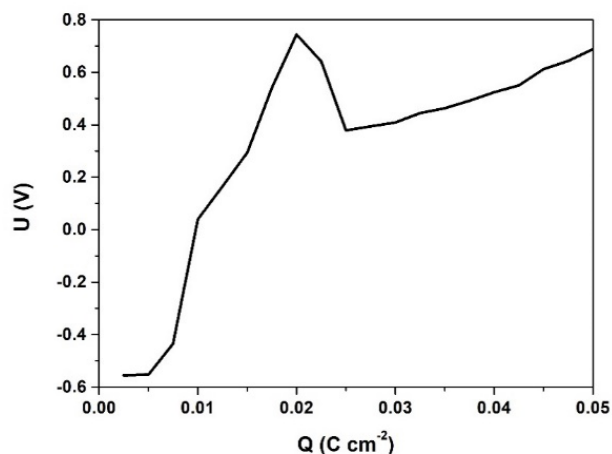


Fig. 3. Kinetic curve for anodizing of antimony, with preliminary deposited  $\text{Sb}_2\text{O}_3$  layers with 7 nm thickness in  $0.12 \text{ mol dm}^{-3}$  aqueous solution of  $\text{K}_3\text{PO}_4$ .

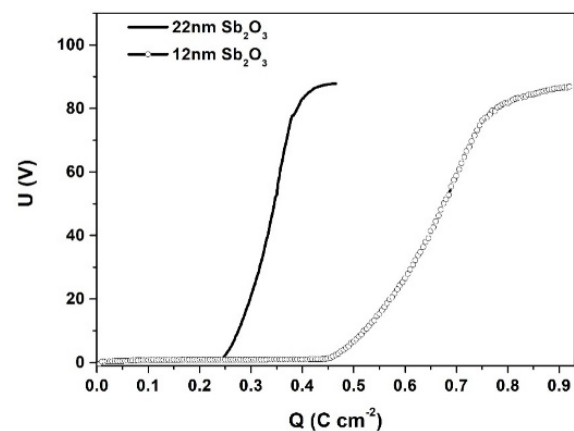


Fig. 4. Kinetic curves for anodizing of antimony with preliminary deposited  $\text{Sb}_2\text{O}_3$  layers with 12 and 22 nm thickness in  $0.12 \text{ mol dm}^{-3}$   $\text{K}_3\text{PO}_4$  aqueous solution.

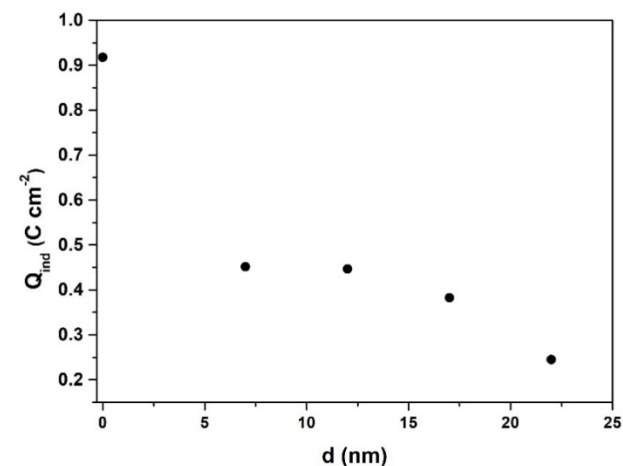


Fig. 5. Dependence of the charge density passed till the end of the induction period  $Q_{ind}$  on the thickness of the  $\text{Sb}_2\text{O}_3$  coating for anodizing in a  $0.12 \text{ mol dm}^{-3}$  aqueous solution of  $\text{K}_3\text{PO}_4$ .

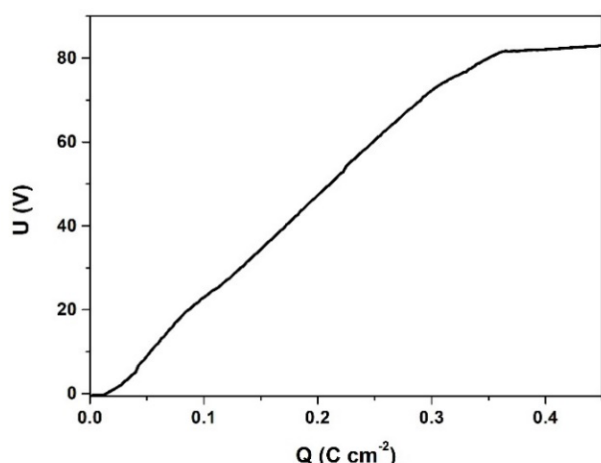


Fig. 6. Kinetic curve for anodizing of antimony preliminary coated with a 100 nm thick  $\text{Sb}_2\text{O}_3$  layer in a  $0.12 \text{ mol dm}^{-3}$  aqueous solutions of  $\text{K}_3\text{PO}_4$ .

mechanism could be as proposed in [22]. Dissolution products block a portion of the electrode surface, causing an increase in current density through the free surface. When it reaches a certain value, the induction period ends. At this point, the voltage becomes grow notably, due to the thickening of the already formed oxide layer.

The preliminary vacuum deposited  $\text{Sb}_2\text{O}_3$  thin (near 7 nm) layers change the kinetic curve shapes, since the kinetic curves initiations in these cases coincide with the end of the hump areas (i.e. near *point 3* in Fig. 2).

In the cases of preliminary vacuum deposited  $\text{Sb}_2\text{O}_3$  layers with thicknesses between 12 and 22 nm, the respective anodization kinetic curves initiations correspond the interval enclosed between points 3 and 4 (Fig. 2), so that for thicker coatings, the kinetic curve initiations are closer to point 4 (Fig. 2). Consequently, the anodization kinetic curve could start even after point 4, when the preliminary  $\text{Sb}_2\text{O}_3$  layer is sufficiently thick. However, such cases were not observed during the experiments. The probable reason is the strong non-stoichiometry and instability of the vacuum-thermally deposited  $\text{Sb}_2\text{O}_3$  layers [30, 31]. As a result, the kinetic curves for the anodizing of antimony electrodes coated with a  $\text{Sb}_2\text{O}_3$  layer always begin from zero voltage even at high thickness values (Fig. 6). These effects become weaker at higher current densities and eventually, the induction period could even disappear at rather high current densities.

## CONCLUSIONS

The preliminary  $\text{Sb}_2\text{O}_3$  layer vacuum-thermal deposition of the Sb electrodes significantly affects the shape of the kinetic curves, acquired during the anodization in  $\text{K}_3\text{PO}_4$  aqueous solutions. The thicker preliminary deposited  $\text{Sb}_2\text{O}_3$  layers result in shortening of the initial induction periods. These periods could completely disappear, when the  $\text{Sb}_2\text{O}_3$  layers are sufficiently thick. This phenomenon, along with the dependence of the kinetic curve slope and the layer band gap width on electrolyte concentration, suggests that the alteration in the dielectric properties of the thin film formed on the electrode surface plays much more significant role in the kinetics of anodizing than previously believed.

## Acknowledgements

*This work is developed as part of contract No BG-RRP-2.004-0002-C01, project name: BiOrgaMCT, Procedure BG-RRP-2.004 „Establishing of a network of research higher education institutions in Bulgaria“, funded by BULGARIAN NATIONAL RECOVERY AND RESILIENCE PLAN.*

## REFERENCES

1. I.A. Ammar, A. Saad, Anodic oxide film on antimony: I. Role of experimental conditions and growth kinetics in acid media, *J. Electroanal. Chem.*, 30, 1971, 395-406.
2. A.A. Girginov, V.M. Kalfova, I.A. Kanazirski, S.M. Ikonopisov, Anodizing of antimony in sulfuric acid solutions, *Russ. J. Electrochem.*, 26, 1990, 110-112.
3. S.M. Ikonopisov, V.M. Kalfova, A. Girginov, High voltage anodizing of antimony, *Compt. rend. Acad. bulg. Sci.*, 41, 8, 1988, 89-91.
4. A.S. Mogoda, W.A. Badawy, M.M. Ibrahim, Role of anions in the anodic behaviour of antimony in aqueous solutions, *Bull. Electrochem.*, 11, 1995, 231.
5. A. El-Rahman El-Sayed, A.M. Shaker, H.G. El-Kareem, Anodic behaviour of antimony and antimony-tin alloys in alkaline solutions, *Bull. Chem. Soc. Jpn.*, 76, 2003, 1527-1535.
6. S. Liu, J. Feng, X. Bian, J. Liu, H. Xu, The morphology-controlled synthesis of a nanoporous-antimony anode for high-performance sodium-ion batteries, *Energy*

- Environ. Sci., 9, 2016, 1229-1236.
7. W.D. McCulloch, X. Ren, M. Yu, Z. Huang, Y. Wu, Potassium-ion oxygen battery based on a high capacity antimony anode, *ACS Appl. Mater. Interfaces*, 7, 2015, 26158-26166.
  8. Q. Sun, Z. Cao, Z. Ma, J. Zhang, W. Wahyudi, T. Cai, H. Cheng, Q. Li, H. Kim, E. Xie, L. Cavallo, Y.-K. Sun, J. Ming, Discerning Roles of Interfacial Model and Solid Electrolyte Interphase Layer for Stabilizing Antimony Anode in Lithium-Ion Batteries, *ACS Materials Lett.*, 4, 11, 2022, 2233–2243. <https://doi.org/10.1021/acsmaterialslett.2c00679>
  9. Q. Sun, Z. Cao, Z. Ma, J. Zhang, H. Cheng, X. Guo, G.-T. Park, Q. Li, E. Xie, L. Cavallo, Y.-K. Sun, J. Ming, Dipole–Dipole Interaction Induced Electrolyte Interfacial Model To Stabilize Antimony Anode for High-Safety Lithium-Ion Batteries, *ACS Energy Lett.*, 7, 10, 2022, 3545-3556. <https://doi.org/10.1021/acsenerylett.2c01408>
  10. Q. Sun, Z. Cao, Z. Ma, J. Zhang, W. Wahyudi, G. Liu, H. Cheng, T. Cai, E. Xie, L. Cavallo, Q. Li, J. Ming, Interfacial and Interphasial Chemistry of Electrolyte Components to Invoke High-Performance Antimony Anodes and Non-Flammable Lithium-Ion Batteries, *Adv. Funct. Mater.*, 33, 1, 2023, 2210292. <https://doi.org/10.1002/adfm.202210292>
  11. L. Zhou, Z. Cao, J. Zhang, H. Cheng, G. Liu, G.-T. Park, L. Cavallo, L. Wang, H.N. Alshareef, Y.-K. Sun, J. Ming, Electrolyte-Mediated Stabilization of High-Capacity Micro-Sized Antimony Anodes for Potassium-Ion Batteries, *Adv. Mater.*, 33, 8, 2021, 2005993. <https://doi.org/10.1002/adma.202005993>
  12. W. Luo, J. Ren, W. Feng, X. Chen, Y. Yan, N. Zahir, Engineering Nanostructured Antimony-Based Anode Materials for Sodium Ion Batteries, *Coatings*, 11, 10, 2021, 1233. <https://doi.org/10.3390/coatings11101233>
  13. J. He, Y. Wei, T. Zhai, H. Li, Antimony-based materials as promising anodes for rechargeable lithium-ion and sodium-ion batteries, *Mater. Chem. Front.*, 2, 2018, 437-455. DOI: 10.1039/C7QM00480J
  14. N. Serrano, J.M. Díaz-Cruz, C. Ariño, M. Esteban, Antimony- based electrodes for analytical determinations, *TrAC Trends Analyt. Chem.*, 77, 2016, 203-213. <https://doi.org/10.1016/j.trac.2016.01.011>
  15. V. Urbanová, K. Vytřas, A. Kuhn, Macroporous antimony film electrodes for stripping analysis of trace heavy metals, *Electrochem. Commun.*, 12, 1, 2010, 114-117.
  16. S. Ikonopisov, A. Girginov, V. Tsochev, Anodic Formation of Barrier Films on Antimony, *Compt. rend. Acad. bulg. Sci.*, 25, 1972, 653-656.
  17. A. Girginov, E. Klein, V. Kalfova, S. Ikonopisov, Anodic Film Formation on Antimony in Phosphate Electrolytes, *B. Electrochem.*, 4, 7, 1988, 631-633.
  18. M. Bojinov, I. Kanazirski, A. Girginov, Anodic film growth on antimony in H<sub>3</sub>PO<sub>4</sub> solutions, *Electrochimica Acta*, 40, 1995, 873-878.
  19. S. Ikonopisov, Anodization of molybdenum in glycol-borate electrolyte— A peculiar kinetics of insulating film formation, *Electrodep. Surface Treat.*, 1, 1973, 305-317.
  20. O.E. Linarez Perez, M.A. Perez, M.L. Teijelo, Characterization of the anodic growth and dissolution of antimony oxide films, *J. Electroanal. Chem.*, 632, 2009, 64-71.
  21. A. Girginov, S. Ikonopisov, Some general characteristics of anodizing of antimony to high voltages in various electrolytes, *Russ. J. Electrochem.*, 10, 4, 1974, 638-641.
  22. I.G. Angelov, C.A. Girginov, E. Klein, Growth and dissolution of anodic antimony oxide in oxalic acid electrolytes, *Bulg. Chem. Commun.*, 43, 2011, 144-149.
  23. S.S. Abdel Rehim, H.H. Hassan, M.A. Amin, Galvanostatic anodization of pure Al in some aqueous acid solutions Part I: Growth kinetics, composition and morphological structure of porous and barrier-type anodic alumina films, *J. Appl. Electrochem.*, 32, 2002, 1257-1264. <https://doi.org/10.1023/A:1021662814303>
  24. E.S.M. Goh, T.P. Chen, C.Q. Sun, Y.C. Liu, Thickness effect on the band gap and optical properties of germanium thin films, *J. Appl. Phys.*, 107, 2010, 024305-024305-5.
  25. J.-P. Xu, R.-J. Zhang, Y. Zhang, Z.-Y. Wang, L. Chen, Q.-H. Huang, H.-L. Lu, S.-Y. Wang, Y.-X. Zheng, L.-Y. Chen, The thickness-dependent band gap and defect features of ultrathin ZrO<sub>2</sub> films studied by spectroscopic ellipsometry, *Phys. Chem. Chem. Phys.*, 18, 2016, 3316-3321.
  26. M. Pandiaraman, N. Soundararajan, C. Vijayan, Effect of thickness on the optical band gap of silver telluride thin films, *J. Ovonic Res.*, 7, 2011, 21-27.
  27. P. Tyagi, A.G. Vedeshwar, Grain size dependent optical band gap of CdI<sub>2</sub> films, *Bull. Mater. Sci.*, 24,

- 2001, 297-300.
28. P.K. Basu, E. Bontempti, S. Madji, H. Saha, S. Basu, Variation of optical band gap in anodically grown nanocrystalline ZnO thin films at room temperature—effect of electrolyte concentrations, *J. Mater Sci: Mater. Electron.*, 20, 2009, 1203.
29. E. Lilov, V. Lilova, S. Nedev, Optical band gap dependence on the oxalic acid concentration of antimony anodic oxide films, *Bulg. Chem. Commun.*, 48, 2016, 17-20.
30. N. Tigău, Structural and electrical properties of Sb<sub>2</sub>O<sub>3</sub> thin films, *Rom. J. Phys.*, 53, 1–2, 2008, 203-208.
31. N. Tigău, V. Ciupina, G. Prodan, G. I. Rusu, C. Gheorghies, E. Vasile, The influence of heat treatment on the electrical conductivity of antimony trioxide thin films, *J. Optoelectron. Adv. Mater.*, 5, 2003, 907-912.